

ORIGINAL RESEARCH PAPER

Electrospinning Nanofibers Gelatin scaffolds: Nanoanalysis of properties and optimizing the process for tissue engineering functional

Mohammad Jalili¹, Abolfazl Mozaffari^{1,*}, Mazeyar Gashti² and Masoud Parsania³

¹ Department of Textile Engineering, Yazd Branch, Islamic Azad University, Yazd, Iran

² Research and Development Laboratory, PRE Labs Inc., 3302 Appaloosa Road, Unit 3, Kelowna, British Columbia, Canada

³ Department of Microbiology, Faculty of Medicine, Tehran Medical Sciences, Islamic Azad University, Tehran, Iran

Received: 2019-06-12

Accepted: 2019-09-06

Published: 2019-09-20

ABSTRACT

Electrospinning has been recognized as an efficient technique for the fabrication of polymer nanofibers. Recently, various polymers have successfully been electrospun into ultrafine fibers. Electrospinning is an extremely promising method for the preparation of tissue engineering scaffolds. In this study, nanofibers gelatin was electrospun at 20% v/v optimized content. To produce gelatin nanofibers optimally, production parameters need to be investigated. In the electrospinning, device (voltage and distance) parameters were determined to be effective; as a result, these parameters were researched and the influences of electrospinning device parameters (voltage & distance) on properties of gelatin nanofibers were evaluated. These parameters affected the diameter size, uniformity, hydrophilicity and thermal degradation of electrospun gelatin nanofibers. All of these properties were examined by SEM, FTIR, CA, BET, XRAY and TGA tests and finally optimum gelatin nanofibers can be used in many applications including cell culture, drug delivery and tissue engineering.

Keywords: Electrospinning; Gelatin; Morphology; Nanofibers; Tissue Engineering

© 2019 Published by Journal of Nanoanalysis.

How to cite this article

Jalili M, Mozaffari A, Gashti M, Parsania M. Electrospinning Nanofibers Gelatin scaffolds: Nanoanalysis of properties and optimizing the process for tissue engineering functional. J. Nanoanalysis., 2019; 6(4): 289-298. DOI: 10.22034/jna.***

INTRODUCTION

Biodegradable synthetic polymer materials such as poly (glycolic acid), poly (lactic acid), and their copolymers, poly (p-dioxanone), and copolymers of trimethylene carbonate and glycolide have been used in a number of clinical applications. Natural, biodegradable polymer materials are derived from certain proteins such as collagen, gelatin, and albumin and certain polysaccharides such as cellulose, hyaluronate, chitin, and alginate. These Polymer materials are different in their molecular weight, polydispersity, crystallinity, thermal transition, and different degradation rate which

would strongly affect polymer scaffold properties. For example, polymer hydrophobicity and crystallinity degree can affect the cellular phenotype, whereas deflection in the surface charges will affect the cellular spreading. This can be the reason for changes in cellular activities [1],[2].

Gelatin is a natural polymer with strong polarity. It has molecular chains connected through strong hydrogen bonds, constituting a 3D macromolecular network (double or triple helix) with reduced mobility [3]. Because of its many merits such as its biological origin, biodegradability, biocompatibility and commercial availability at relatively low cost,

* Corresponding Author Email: mozaffari@iauyazd.ac.ir



gelatin has been widely used in the pharmaceutical and medical fields [4],[5].

One of the main reasons for using Gelatin compared to collagen is that the triple helical structure is broken and thus the R-G-D sequence is much better exposed which may be somehow hidden in the collagen triple helical structure. Therefore, using Gelatin instead of collagen can be beneficial because it is denatured and short, and it promotes cell adhesion, migration, differentiation, and proliferation in the field of tissue engineering applications [[6],[7],[8]]. In some previous studies, scaffolds including Gelatin were prepared to obtain desired porosity and biocompatibility for soft tissue engineering [9] or artificial skin engineering [10],[11].

On the other hand, gelatin is a natural biopolymer derived from collagen by controlling hydrolysis.

Electrospinning is a simple and versatile technique to generate nano to micrometer fibrous structures which are very similar to the natural fibrillar extracellular matrix (ECM) [12],[13]. This process involves applying an electric field to draw solution continuously from the needle to the collector plate [14],[15]. Morphology of electrospun fibers depends on the solution, device and environmental parameters [4],[16],[8].

A great number of studies have been conducted on electrospinning of gelatin to produce nanofibers. In this regard, Oktan et al. investigated the influence of the process parameters on the properties of electrospun gelatin. They found that zeta potential and the diffusion coefficients were higher for dispersion electrospun gelatin than normal gelatin [2].

In another study, Huang et al. used a different organic solvent; 2,2,2 trifluoro ethanol in gelatin. Their study led to gelatin nanofibers in the range of 100-340 nm. More recently, Chang has used formic acid as a solvent in electrospinning of gelatin and produced nanofibers ranging from 70 to 170 nm [6].

On the other hand, some researchers blended gelatin with other polymers and evaluated the spinnability of blended nanofibers. Zhang et al. produced nanofiber composites of gelatin/PCL. Their resulted nanofibers showed improved mechanical properties in comparison with pure gelatin [3]. Ghasemi used the same scaffold for nerve tissue engineering. MTS assay and SEM results showed that the biocomposite of PCL/gelatin 70:30 nanofibrous scaffolds enhanced the nerve differentiation and proliferation compared to PCL nanofibrous scaffolds and acted as a positive

cue to support neurite outgrowth. It was found that the direction of nerve cell elongation and neurite outgrowth of aligned nanofibrous scaffolds was parallel to the direction of the fibers [18]. The resulting nanofibrous scaffolds exhibited smooth surface and high porous structure. Blending PLGA with gelatin enhanced the hydrophilicity but decreased the average fiber diameter and the mechanical properties of the scaffolds under the same electrospinning condition [7].

In other research, Nagihan Okutan et al. electrospun gelatin in different concentrations, rates and voltages. Their findings showed that the range of nanofiber diameters increased with the applied voltage [1].

However, a few studies have focused on the effects of electrospinning process parameters on morphology, crystallinity and physical properties of gelatin nanofibers.

MATERIALS AND METHODS

Preparation, characterization and quantification of nG(nano fiber Gelatin)

According to the previous studies, acetic acid is a solvent for solving gelatin in water. As a result of the presence of acetic acid, the decomposition process slows down the polymer structure and increases the viscosity of the polymer solution to prevent the bead-like and uneven structure nano gelatin fibers (1). The solutions with 20% (v/v) gelatin content were prepared by dissolving 20% gelatin powder (type A, Bio Reagent with code G1890 from porcine skin was purchased from SIGMA ALDRICH) in 5cc acetic acid (66%) (also purchased from SIGMA ALDRICH) and 5cc deionized distilled water (from HYDRO PARS KIMIA of IRAN). Then the solution was stirred at room temperature for 1h to obtain a homogenous solution. This solution was later used for electrospinning.

Electrospinning of gelatin nanofibers

The polymer solution was taken in a 3 ml syringe with a blunt-end needle and was loaded in the electrospinning setup. The polymer solution was electrostatically drawn from the tip of the needle by applying a high voltage between the tip of the needle and the grounded target (collector) using high-voltage power supply. The flow rate of the solution was kept at 0.6 ml/h, we used three voltages (10 kV, 12 kV, 15 kV) and the distance between the needle tip and collector (air gap) was set at 10, 15, 20 cm and nanofibers were collected

onto an aluminum (Al) sheet. The electrospinning apparatus was from Fanavaran nano-meghyas Co. (Iran). Nano scaffolds of gelatin were electrospun using the above-mentioned standardized electrospinning conditions many times. Finally, nanofibers were spun at room temperature for 45 min [3].

Equipment

The morphology of Gelatin nanofibrous scaffolds (Gns) was investigated using SEM (XL30 Philips microscope) with Atlas Tescan software for image analysis. Fourier transform infrared spectroscopy (FTIR) was used to identify the chemical structure of nanofibers. The spectral scan was carried out from 600 to 4000 cm^{-1} and 4 cm^{-1} resolutions using an IR-spectrometer (IRAFFINITY-1 (SHIMADZU Company)). Thermogravimetric analysis of the scaffolds was carried out using a TG/DTA instrument (Pyris Diamond SII, Perkin Elmer Thermo Analyzer, USA) at a range of 50–600 °C. Wettability of the scaffolds was measured using a water contact angle system supported by video cam equipment (Perkin Elmer Spectrum RX-1, USA). Continuous recording of contact angles was done from time zero and constant contact angle values were obtained in order to eliminate any influence of subsequent perfusion flow through the nanofibrous scaffolds. The BET Surface Area Measurement technique, the

most frequent method for determination of specific surface area of porous materials, was carried out using the nitrogen adsorption (Mi-cromeritics Gemini III 2375, USA) and The crystallinity of the gelatin nanofibers was evaluated from wide-angle X-ray diffractograms recorded with a Philips X'Pert Pro Multipurpose X-ray Diffractometer operating at 40 kV and 40 mA.

RESULTS AND DISCUSSIONS

Spinnability and fiber diameter

As it can be seen from SEM images of nanofibers scaffold, 9 samples were electrospun in different device conditions (voltage & distance between nozzle and collector (TCD)). In the current study, 3 different voltages (10, 12, 15 kV) and 3 different distances (10, 15, 20 CM) were used, SEM images can be seen in Fig 1.

Some researchers such as Sander et al. used acetic acid in their solvent, which shows the effect of acetic acid morphology on electrospinning fibers. In a polymer solution containing acetic acid, there is little electrical conductivity, which can increase the electrical conductivity of the solution by increasing the acetic acid. Moreover, Lien et al. found that by increasing the concentration of acetic acid solution, the diameter of the fibers decreased with electroplating of caprolactane [13]. As a result, we also used 50/50 acetic acid-water solution in our study. At a voltage of 10 kV and distance of

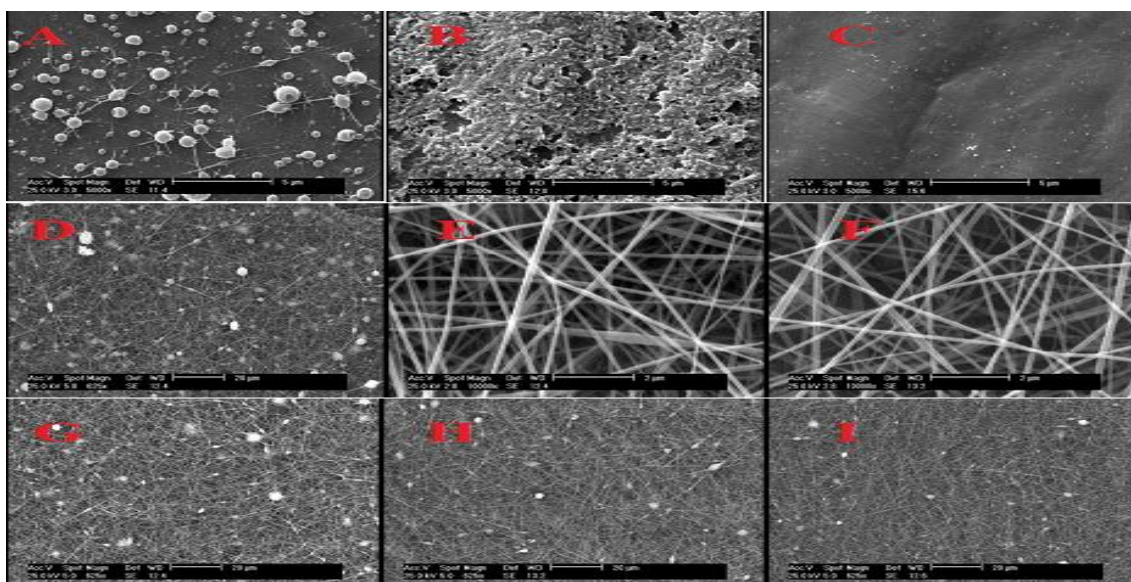


Fig. 1. A:Voltage :10 kV ,TCD:10 cm-B:Voltage:10 kV,TCD:15cm-C:Voltage:10 kV,TCD:20cmD:Voltage:12 kV ,TCD:10 cm-E:Voltage :12 kV,TCD:15cm-F:Voltage:12 kV ,TCD:20 cm G:Voltage:15 kV,TCD:10 cm-H:Voltage15 kV,TCD:15 cm-I:Voltage:15 kV,TCD:20 cm

Table 1. Different device conditions used for scaffold fabrication with obtained nanofiber morphology and average nanofiber diameter

Sample No	Voltage & Distance	Average Diameter	Standard Deviation	Fiber morphology obtained
A	10-10	116.3	40.03	Nanofibres with high amount of beads
B	12-10	118.4	14.54	Nanofibres with Less amount of beads
C	15-10	139.9	29.74	Nanofibres with Less amount of beads
D	10-15	0	0	No fibers
E	12-15	101.9	11.8	Nanofibers with minimum of beads and more uniformity
F	15-15	129.8	22.53	Nanofibers with minimum of beads and uniformity
G	10-20	0	0	No fibers
H	12-20	79.63	9.69	Bead-free nanofibers
I	15-20	138.7	29.48	Nanofibers with lower beads and uniformity
Ideal item (E)	12-20	101.9	11.8	

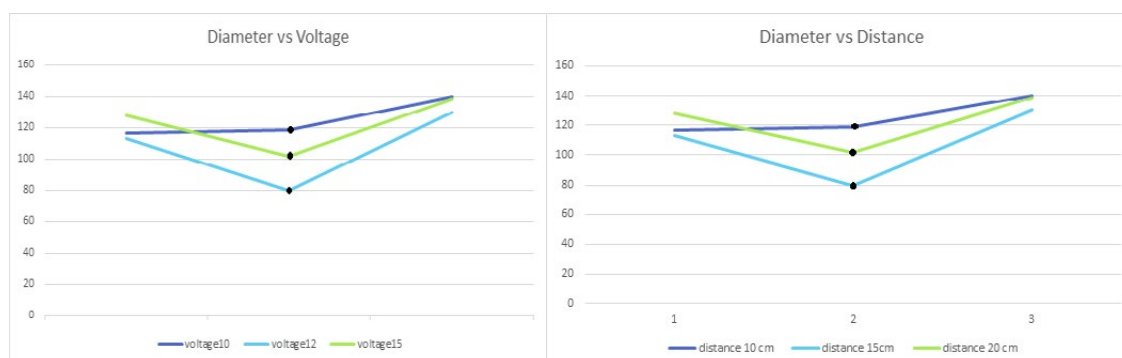


Fig. 2. diagram of diameter vs. voltage and distance

10 cm, highly bead fibers can be observed (Fig. A). However, when the distance was increased to 15 and 20 cm, nanofibers did not form. This can be due to low voltage, which increases the gap between the nozzle and the collector (Figs. D & G). Figures B and C show 10 centimeters TCD in different voltages. In voltage of 20 kV, nanofibers in Fig C showed fewer beads than in Fig B; hence, the number of beads decreases with the increase in the voltage in the scaffold, which can be due to the low flow rate, which is formed by increasing the steady state flow rate in the fibers and the scaffold. The average standard deviation of the nanofibers is 10-15% and their range varies between 79 and 139 [13]. Fong et al. found that the viscoelasticity, jet charge density and solvent stress level were the factors affecting the formation of bead. As shown in Fig. H and I, at the voltage of 15 kV and TCD of 15- 20 cm, the fibers are produced with lower beads and more uniformity by increasing TCD, which can be reduced due to the viscoelastic factor. At distances of 15 cm and voltages of 15 and 20 kV, the result is as depicted in Figs. E and F. The nanofibers are formed with minimum number of beads and more uniformity, with fibers having

a lower diameter in 20 kV than 15 kV, which is probably due to the effect of increased viscosity and the corresponding electrical forces [19]. Table 1 shows different device conditions used for scaffold fabrication with obtaining nanofiber morphology and average nanofiber diameter.

The diagram in Fig. 2 depicts the average diameter of the fibers on the distance between the needle tip and the collector. We used 3 distances, 10, 15 and 20 cm, in this diagram, which can be achieved by selecting the appropriate distance from the minimum beads and the inner and outer layers of the joints, which increases the strength of the scaffold [11]. On the other hand, by increasing the distance between the needle tip and the collector, it is possible to electrospinning the fibers with a smaller diameter[4]With electrospinning gelatin in the three mentioned distances, we found that at 20 cm in each of the three voltages, fibers with a smaller diameter were produced. By integrating two voltage and distance diagrams, the optimal conditions for gelatin electrospinning to obtain the thinnest fibers with the strength and ideal conditions were determined, including a voltage of 12 kV at a distance of 20 cm.

FTIR spectroscopy

As shown in the Fig. 3, the FT-IR spectrum of raw gelatin and nanofibers scaffold showed many bands that were the same or close to each other, such as at 3443 cm⁻¹ due to N-H stretching of amide bond, C-H stretches at 2925 cm⁻¹, C=O stretches at 1635-1651 cm⁻¹, 1444-1449 cm⁻¹ arise from C-C bond or also 610-66 cm⁻¹ related to C-H bond, respectively.

Significant peaks of gelatin are clearly shown in both Fig. A and Fig. B. In the FTIR of Gelatin composite in Guatam's research, all the above peaks were represented [20]. It is important that combining gelatin with acetic acid and electrospinning them did not affect its morphology and bonds. All the peaks and their reactions can be seen in Table 2 [21], [22], [23]. Prystupa and Muyonga and also Ki et al. reported the amide I band at 1650 cm⁻¹, which was attributable to both a random coil and a-helix conformation of gelatin [24], [25], [26].

Among them, the amide I band is caused by C-O stretching vibrations of the peptide linkages in the backbone of protein and the amide II band is caused by the combination of N-H in plane bending and C-N stretching vibrations and N-H out-of-plane wagging at 610 cm⁻¹ [20], [27]. Comparing the two FTIR diagrams, sample A has higher peaks than sample B.

The CA measurements

Generally, the hydrophilic/hydrophobic characteristics of a scaffold are important in tissue culture and can affect the initial cell adhesion and cell migration to a higher extent [28] desirable biocomposites for tissue-engineering applications. Random and aligned PCL/gelatin biocomposite scaffolds were fabricated by varying the ratios of PCL and gelatin concentrations. Chemical and mechanical properties of PCL/gelatin nanofibrous scaffolds were measured by FTIR, porometry, contact angle and tensile measurements, while the in vitro biodegradability of the different nanofibrous scaffolds were evaluated too. PCL/gelatin 70:30 nanofiber was found to exhibit the most balanced properties to meet all the required specifications for nerve tissue and was used for in vitro culture of nerve stem cells (C17.2 cells. According to previous literature, hydrophobic surfaces lead to lower cell adhesion in the initial step of cell

Table 2. ATR-FTIR of Gelatin Peaks and Band Assignments

Peak Position (Cm-1)	Band Assignment
610 -669	C -H
1383	- CH ₃
1444 -1449	C-C Stretch
1635 -1651	Amide I (C=O Stretch)
2925	- CH Stretch
3443	O-H Stretch , NH Stretch

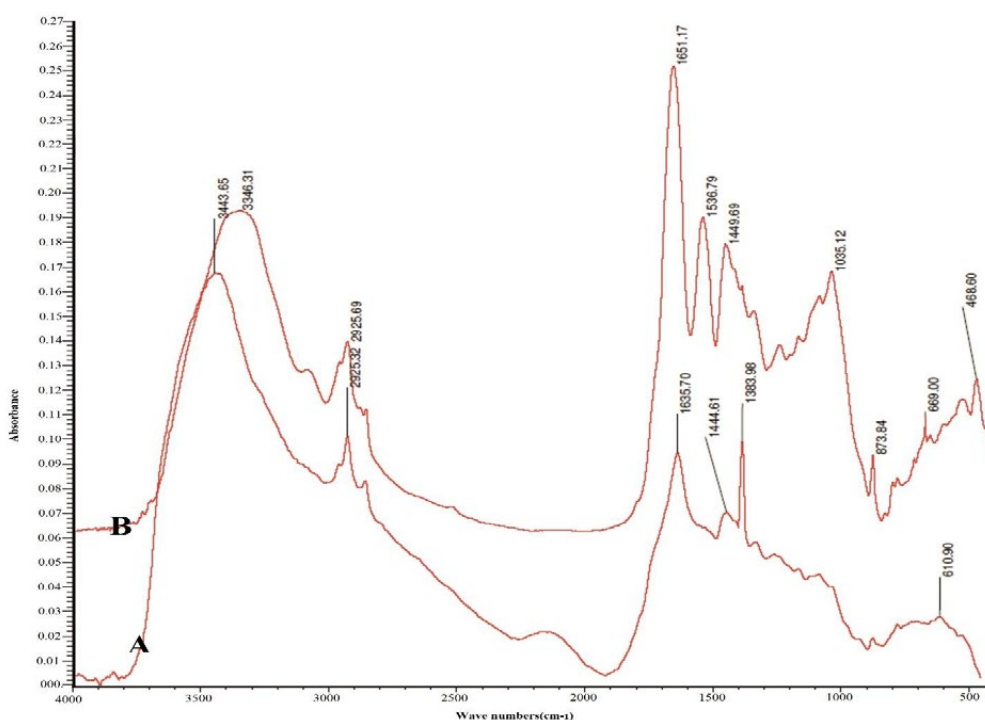


Fig. 3. reports the FTIR spectra of raw gelatin (A) and nano fibers scaffold prepared from acetic acid/water solution (B)

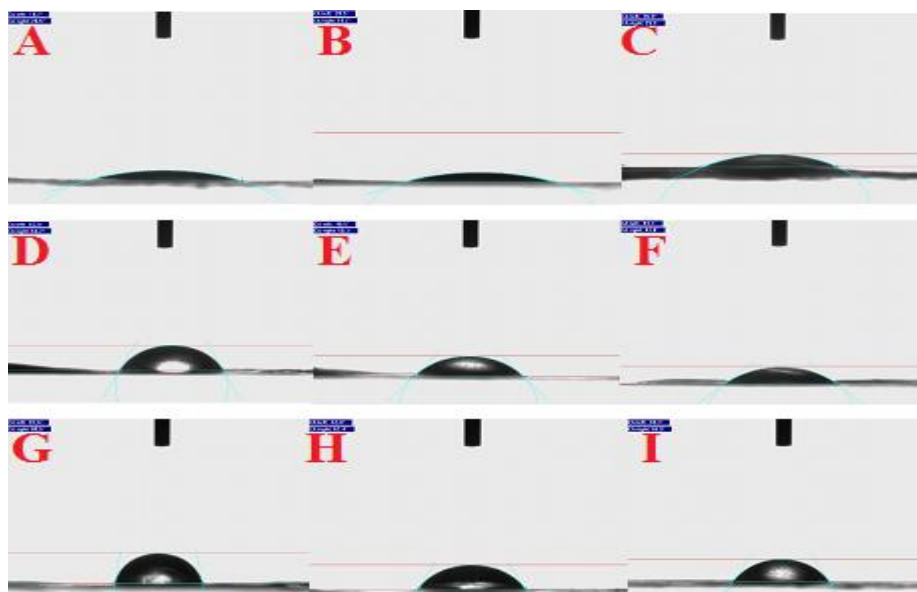


Fig. 4. pictures of water drops on nanofiber network

culture [21]. Because of this, it seems necessary to investigate the wettability of scaffolds and for determination of wettability or hydrophilicity of scaffolds, the contact angle (CA) of electrospun nanofibers must be measured by a surface-analysis instrument. The droplet size was set at 0.5 ml. and three samples were used for each test, the average value of which was reported. As expected, gelatin showed better wettability than other polymers because of its hydrophilic attribute [8]. Ghasemi et al. also represented that the hydrophilicity of PCL/gelatin scaffolds increased with increasing gelatin concentration [19]. Because of this, we used 27%, which has a high concentration in gelatin. Fig. 4 shows the shape of a water drop on the surface of nanofibers Gelatin scaffolds and Table 3 shows the results of contact angle data for different conditions of Gelatin nanofibers (A-I). As it can be seen in Table 3, in all specimens (A-I), increasing the distance (TCD) results in an increase in the hydrophilicity property of the scaffold, increasing the voltage increases the hydrophobicity property of the scaffold. In group 1, either no nanofiber is observed or nanofibers with more beads are observed that have a large difference in the contact angles with other groups, which can be due to non-uniformity of the network and bead distribution. In the second group, ideal and uniform nanofibers were obtained, the contact angle is lower than the third group and has a better hydrophilic property. The contact angle was 63, 46 and 43 in specimen

Table 3. The CA measurements

Group	Sample NO	Average water Contact Angle (°)
1	A	18
	B	19
	C	22
2	D	63
	E	46
	F	43
3	G	76
	H	59
	I	56

D, E and F, respectively. As it can be seen, with increasing the distance, the contact angle of the scaffolds decreases.

Surface area, porosity, and water retention of electrospun nanofibers

Functional characteristics of the prepared scaffolds with respect to tissue engineering were investigated by studying the water vapor permeability, surface area, and pore structure. The BET method has previously been used to measure the surface area of electrospun nanofibers of gelatin. Table 4 shows the BET results of electrospun nanofibers of gelatin. It was observed that all the preparations nanofibrous mats had a comparable permeability. This was anticipated since every mat showed a porous network of entangled electrospun

nanofibers [22]. Surprisingly, an increase in surface area was observed for increasing device conditions (TCD and voltage) of gelatin electrospinning. As there was a decrease in diameter of nanofibers with increasing device conditions of gelatin

electrospinning, an increase in the surface area should have occurred. Hence average pore diameters of the nanofibrous scaffold were also measured using BET. A decrease in pore diameter was observed with increasing the device conditions of gelatin nanofibers scaffold. Nanofibrous mats with similar surface area, pore morphology, porosity, and relevant mechanical properties with potential tunable degradable properties have been developed by merely varying the condition of electrospinning of gelatin [29]. It is possible to control the pore morphology, porosity, and relevant mechanical properties by adjusting their blending ratios and controlling the electrospinning process. These porous fibrous scaffolds hold considerable significance in the tissue engineering related applications [30]. The 3D porous of biomimicking composite fiber of Gt/PCL could have considerable

Table 4. surface and porous properties of electrospun nanofibers

Sample	Mean pore diameter	BET surface area(m ² g ⁻¹)	Pore volume
A	15.22	2.91	3.31
B	15.2	5.15	1.96
C	14.78	5.26	0.08
D	13.43	6.06	5.58
E	9.45	6.39	2.77
F	9.91	9.52	0.48
G	8.23	5.26	5.59
H	7.05	10.22	4.5
I	6.18	17.74	0.61

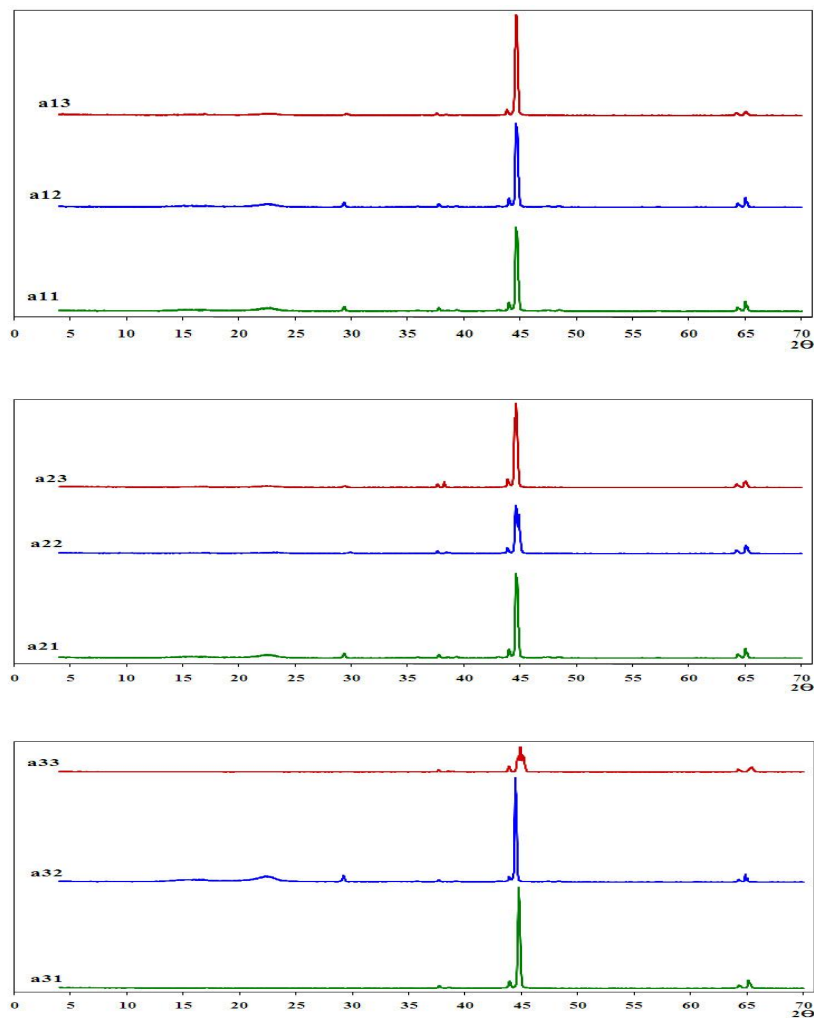


Fig. 5. X-ray diffraction of nanofibers gelatin scaffold

value for applications in developing highly integrated cell–scaffold tissue complexes and other industrial applications [24]. Firstly, cellular can grow to a deeper level inside nanofibers. Second study nano-topographical effect of nanofibers on cell behavior. The third study on behavior of the biodegradable polymers[29],[24]. It is clearly observed from Table 4 that a decrease in pore size corresponds to a decrease in water retention properties of nanofibers [23]. It can be concluded that increasing device conditions increases the surface area and decreases pore diameter and finally decreases the diameter of nanofibers. This finding is also confirmed by SEM images.

X-ray diffractometry(XRD)

X-ray diffraction of nanofibers gelatin scaffold is shown in Fig. 5. Gelatin nanofibers scaffolds show all the characteristic peaks of Gelatin with low and sharp intensity (Fig. 5) that confirmed the crystalline nature of scaffold. Gelatin showed no peak in XRD pattern, which indicates its amorphous nature[20]. This was also reported by Xue and also Ki et al. [24], [31]. However, Gelatin scaffolds showed sharp peak at 2θ of 45° and a relatively low-intensity peak at 38.5° and 65.5° , indicating the semi-crystallinity of gelatin electrospun. The decreased intensity of Gelatin-Pcl peaks indicates the reduction in the degree of crystallinity of the scaffold and this might be due to some interactions between the molecules of crystalline and amorphous gelatin [20], [32]. The absence of a diffraction peak in the XRD pattern of gelatin indicates that gelatin is amorphous [20], [24], [31]. Panzavolta et al. and also Ki et al. reported that in the typical XRD pattern of gelatin, crystalline structure originated from triple helix structure [31], [33] Also Ki also reported that

Table 5. crystallinity percent

Sample	crystallinity percent
A11	35.90
A12	35.90
A13	44.20
A21	35.90
A22	41.79
A23	46.09
A31	32.24
A32	45.38
A33	61.17

Table 6. Thermal properties of the electrospun gelatin nanofibers

No Sample	Wt ^{555°} (R%)	T _{iD} (°C)
1 (powder gelatin)	5.6%	331
2 (Ideal nanofibers)	8%	343

amorphous structures were observed mostly for electrospun nanofiber from gelatin-formic acid (7-12% wt%) solution [31]. Fong et al. found that the viscoelasticity, jet charge density and solvent stress level were the factors affecting the formation of bead. In fact, the fibers are produced with lower beads and more uniformity by increasing TCD which can be reduced due to the viscoelastic factor [19]. Table 5 shows that crystallinity has increased with increasing TCD and voltage, which may be due to the fact that the beads are amorphous.

Thermal degradation (TGA)

TGA was performed on scaffolds to determine the changes in weight in relation to changes in temperature. The thermal properties of gelatin powder and ideal Gelatin electrospun nanofibers scaffold were characterized using TGA curve in the range of 25-555 °C in Fig. 6.

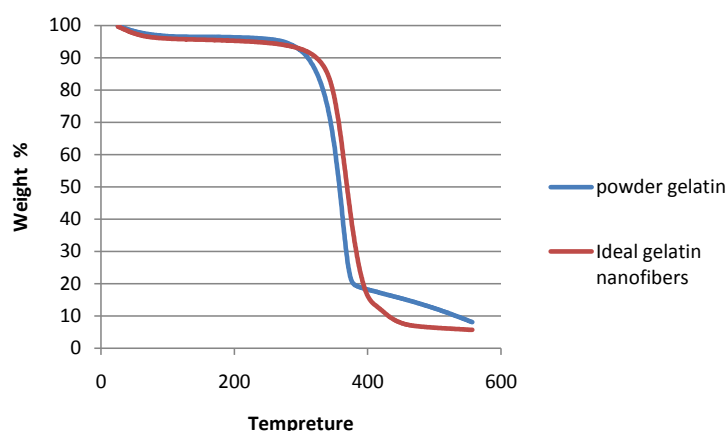


Fig. 6. powder gelatin and ideal Gelatin electrospun nanofibrous

The initial weight loss for both samples occurring in the temperature range 25–150 °C is attributed to the evaporation of water [34], [35]. At about 300°C, an endothermic shoulder was observed and the main weight loss was started, which is related to the helix–coil transition, which means that the electrospinning process does not alter the formation of the characteristic helical structure between the gelatin chains [34]. Weight loss in this temperature range is about 5-6% [36] [37]. The main weight loss for gelatin samples was observed in the temperature range 300 °C – 450 °C, which is likely accompanied by breaking of peptide bonds [35], [37], [38]. The exact mass losses of all scaffolds as measured by TGA were approximately 55% (powder gelatin) and 35% (gelatin Ideal sample).

The powder gelatin and ideal electrospun gelatin nanofibers scaffolds are reported in Table 6. As it can be seen, the mass decomposition temperature in powder gelatin was about 331°C and for gelatin nanofibers was 343 °C but the main decomposition temperature occurred in about 330-345 °C. The ideal gelatin nanofibers had better thermal properties than powder gelatin. This phenomenon was associated with the electrospinning process [39], [40], which is relatively easy crystallization and increased segmental mobility of the fibrous polymers after this electrospinning process [40].

CONCLUSION

The electrospinning of gelatin solutions with acetic acid at different process conditions at room temperature was tested. The results showed the viability to obtain electrospun gelatin in 20% concentration of acetic acid. In the SEM results, sample E with the voltage of 12 kV and distance of 15 cm was the ideal item for electrospinning as it showed minimum beads with more uniformity at smaller diameter, compared with other samples. As there was a decrease in the diameter of nanofibers with changing the process conditions, an increase in the surface area was expected according to BET results. In addition, the XRD results showed higher crystallinity values. Although in FTIR, both gelatin electrospun nanofibers and gelatin powder clearly show significant and similar peaks, it is important to combine gelatin with acetic acid for feasible processability owing to the fact that it does not affect the morphology and chemical properties. According to CA measurement, with increasing distance, the contact angle of the

scaffolds decreased. This means that hydrophilicity or wettability of scaffolds was improved. The ideal gelatin nanofibers sample had an increased thermal stability in comparison with gelatin powder. This phenomenon was associated with the electrospinning process leading to increased crystallization and segmental mobility of the fibrous polymers after this electrospinning process [39], [40]. Finally, with these improvements in gelatin nanofibers scaffold, we will further study the cell adhesion and proliferation for tissue engineering in the future.

CONFLICT OF INTEREST

The authors declare that there is no conflict of interests regarding the publication of this manuscript.

REFERENCES

- [1] J. O. Hollinger and J. P. Schmitz, *Ann. N. Y. Acad. Sci.*, 831, 1 (1997).
- [2] K. J. . Burg, S. Porter, and J. F. Kellam, *Biomaterials*, 21, 23 (2000).
- [3] W. F. Harrington and P. H. Von Hippel, *Adv. Protein Chem.*, 16, (1962).
- [4] E. J. Chong et al., *Acta Biomater.*, 3, 3 (2007).
- [5] R. Murugan and S. Ramakrishna, *Tissue Eng.*, 12, 3 (2006).
- [6] S. R. Son, N. T. B. Linh, H. M. Yang, and B. T. Lee, *Sci. Technol. Adv. Mater.*, 14, 1 (2013).
- [7] X. Zhang, M. R. Reagan, and D. L. Kaplan, *Adv. Drug Deliv. Rev.*, 61, 12 (2009).
- [8] Y. Zhang, H. Ouyang, T. L. Chwee, S. Ramakrishna, and Z. M. Huang, *J. Biomed. Mater. Res. - Part B Appl. Biomater.*, 72, 1 (2005).
- [9] J. Mao, L. Zhao, K. De Yao, Q. Shang, G. Yang, and Y. Cao, *J. Biomed. Mater. Res. A*, 64, 2 (2003).
- [10] H. Liu, J. Mao, K. Yao, G. Yang, L. Cui, and Y. Cao, *J. Biomater. Sci. Polym.*, 15, 1 (2004).
- [11] J. S. Mao, H. F. Liu, Y. J. Yin, and K. De Yao, *Biomaterials*, 24, 9 (2003).
- [12] S. Ramakrishna, K. Fujihara, W. E. Teo, T. Yong, Z. Ma, and R. Ramaseshan, *Mater. Today*, 9, 3 (2006).
- [13] C. Guo, L. Zhou, and J. Lv, *Polym. Compos.*, 21, 7 (2013).
- [14] A. L. Andrad, "Science and technology of polymer nanofibers", John Wiley & Sons, Inc., 2008, 1–424.
- [15] W. K. Son, J. H. Youk, T. S. Lee, and W. H. Park, *Polymer Guildf.*, 45, 9 (2004).
- [16] S. Farris, K. M. Schaich, L. Liu, P. H. Cooke, L. Piergiovanni, and K. L. Yam, *Food Hydrocoll.*, 25, 1 (2011).
- [17] R. Nirmala et al., *Fibers Polym.*, 12, 8 (2011).
- [18] T. Balau Mindru, I. Balau Mindru, T. Malutan, V. Tura, *J. Optoelectronics & Adv. Mat.*, 9, 11 (2007).
- [19] H. Fong, I. Chun, and D. H. Reneker, *Polymer Guildf.*, 40, 16 (1999).
- [20] S. Gautam, A. K. Dinda, and N. C. Mishra, *Mater. Sci. Eng.*, 33, 3 (2013).
- [21] K. Sisson, C. Zhang, M. C. Farach-Carson, D. B. Chase, and J. F. Rabolt, *Biomacromolecules*, 10, 7 (2009).
- [22] I. V. Yaninas, *J. Macromol. Sci. Part C*, 7, 49 (1972).

- [23] Charbel Tengroth, Ulla Gasslander, Fredrik O. Andersson & Sven P. Jacobsson, *J. Pharmaceutical Development and Technology*, 10, 3 (2005).
- [24] C. S. Ki, D. H. Baek, K. D. Gang, K. H. Lee, I. C. Um, and Y. H. Park, *Polymer Guildf.*, 46, 14 (2005).
- [25] Š. Rýglová, M. Braun, and T. Suchý, *Macromol. Mater. Eng.*, 302, 1 (2017).
- [26] M. G. Haugh, M. J. Jaasma, and F. J. O'Brien, *J. Biomed. Mater. Res., Part A*, 89, 2 (2009).
- [27] M. Meskinfam, M. S. Sadjadi, H. Jazdarreh, *World Academy of Sci., Eng. and Tech.*, 76, (2011).
- [28] L. Ghasemi-Mobarakeh, M. P. Prabhakaran, M. Morshed, M. H. Nasr-Esfahani, and S. Ramakrishna, *Biomaterials*, 29, 34 (2008).
- [29] N. Nagiah, L. Madhavi, R. Anitha, N. T. Srinivasan, and U. T. Sivagnanam, *Polym. Bull.*, 70, 8 (2013).
- [30] Y. Z. Zhang, Y. Feng, Z. M. Huang, S. Ramakrishna, and C. T. Lim, *Nanotechnology*, 17, 3 (2006).
- [31] J. Xue et al., *Biomaterials*, 35, 34 (2014).
- [32] S. A. Martel-Estrada, C. A. Martínez-Pérez, J. G. Chacón-Nava, P. E. García-Casillas, and I. Olivas-Armendariz, *Carbohydr. Polym.*, 81, 4 (2010).
- [33] S. Panzavolta, M. Giofrè, M. L. Focarete, C. Gualandi, L. Foroni, and A. Bigi, *Acta Biomater.*, 7, 4 (2011).
- [34] D. M. Correia, J. Padrão, L. R. Rodrigues, F. Dourado, S. Lanceros-Méndez, and V. Sencadas, *Polym. Test.*, 32, 5 (2013).
- [35] S. E. Kim et al., *Biomed. Mater.*, 4, 4 (2009).
- [36] D. Kolbuk, P. Sajkiewicz, K. Maniura-Weber, and G. Fortunato, *Eur. Polym. J.*, 49, 8 (2013).
- [37] I. Rajzer, E. Menaszek, R. Kwiatkowski, J. A. Planell, and O. Castano, *Mater. Sci. Eng. C.*, 44, 183 (2014).
- [38] P. o. Rujitanaroj, N. Pimpha, and P. Supaphol, *Polymer (Guildf.)*, 49, 21 (2008).
- [39] Z. X. Meng et al., *Colloids Surfaces B Biointerfaces*, 84, 97 (2011).
- [40] X. Y. Yuan, Y. Y. Zhang, C. Dong, and J. Sheng, *Polym. Int.*, 53, 11 (2004).